




Glycine Amidinotransferase (GATM), Renal Fanconi Syndrome, and Kidney Failure

Markus Reichold,¹ Enriko D. Klootwijk,² Joerg Reinders,³ Edgar A. Otto,⁴ Mario Milani,⁵ Carsten Broeker,¹ Chris Laing,² Julia Wiesner,¹ Sulochana Devi,⁶ Weibin Zhou,⁶ Roland Schmitt,¹ Ines Tegtmeyer,¹ Christina Sterner,¹ Hannes Doellerer,¹ Kathrin Renner,⁷ Peter J. Oefner,³ Katja Dettmer,³ Johann M. Simbuerger,³ Ralph Witzgall,⁸ Horia C. Stanescu,² Simona Dumitriu,² Daniela Iancu,² Vaksha Patel,² Monika Mozere,² Mehmet Tekman,² Graciana Jaureguiberry,² Naomi Issler,² Anne Kesselheim,² Stephen B. Walsh,² Daniel P. Gale ,² Alexander J. Howie,² Joana R. Martins,⁹ Andrew M. Hall,⁹ Michael Kasgharian,¹⁰ Kevin O'Brien,¹¹ Carlos R. Ferreira,¹¹ Paldeep S. Atwal,¹² Mahim Jain,¹³ Alexander Hammers,¹⁴ Geoffrey Charles-Edwards,¹⁵ Chi-Un Choe,¹⁶ Dirk Isbrandt,¹⁷ Alberto Cebrian-Serrano,¹⁸ Ben Davies ,¹⁸ Richard N. Sandford,¹⁹ Christopher Pugh,²⁰ David S. Konecki,²¹ Sue Povey,²² Detlef Bockenhauer ,² Uta Lichter-Konecki,²³ William A. Gahl,¹¹ Robert J. Unwin,² Richard Warth ,¹ and Robert Kleta ²

Due to the number of contributing authors, the affiliations are listed at the end of this article.

ABSTRACT

Background For many patients with kidney failure, the cause and underlying defect remain unknown. Here, we describe a novel mechanism of a genetic disorder characterized by renal Fanconi syndrome and kidney failure.

Methods We clinically and genetically characterized members of five families with autosomal dominant renal Fanconi syndrome and kidney failure. We performed genome-wide linkage analysis, sequencing, and expression studies in kidney biopsy specimens and renal cells along with knockout mouse studies and evaluations of mitochondrial morphology and function. Structural studies examined the effects of recognized mutations.

Results The renal disease in these patients resulted from monoallelic mutations in the gene encoding glycine amidinotransferase (GATM), a renal proximal tubular enzyme in the creatine biosynthetic pathway that is otherwise associated with a recessive disorder of creatine deficiency. *In silico* analysis showed that the particular GATM mutations, identified in 28 members of the five families, create an additional interaction interface within the GATM protein and likely cause the linear aggregation of GATM observed in patient biopsy specimens and cultured proximal tubule cells. GATM aggregates-containing mitochondria were elongated and associated with increased ROS production, activation of the NLRP3 inflammasome, enhanced expression of the profibrotic cytokine IL-18, and increased cell death.

Conclusions In this novel genetic disorder, fully penetrant heterozygous missense mutations in GATM trigger intramitochondrial fibrillary deposition of GATM and lead to elongated and abnormal mitochondria. We speculate that this renal proximal tubular mitochondrial pathology initiates a response from the inflammasome, with subsequent development of kidney fibrosis.

J Am Soc Nephrol 29: 1849–1858, 2018. doi: <https://doi.org/10.1681/ASN.2017111179>

Received November 13, 2017. Accepted February 27, 2018.

M.R., E.D.K., J.R., E.A.O., W.A.G., R.J.U., R.W., and R.K. contributed equally to this work.

Published online ahead of print. Publication date available at www.jasn.org.

Correspondence: Dr. Richard Warth, Medical Cell Biology,

University of Regensburg, Universitaetsstrasse 31, 93053 Regensburg, Germany, or Dr. Robert Kleta, University College London, Centre for Nephrology, Royal Free Hospital, London NW3 2PF, United Kingdom. Email: richard.warth@ur.de or r.kleta@ucl.ac.uk

Copyright © 2018 by the American Society of Nephrology

CKD is a worldwide health problem, and it comprises heterogeneous disorders affecting kidney structure and function.¹ The underlying pathogenesis is complex and in many patients, involves genetic predisposition.

Here, we describe in five extended families a novel form of autosomal dominant kidney disease. The disease is characterized by renal tubular Fanconi syndrome early in life followed by progression to renal glomerular failure in middle adulthood. All of our patients show monoallelic mutations in the gene *glycine amidinotransferase* (*GATM*) that create an additional protein-protein interaction surface at which the protein multimerizes, leading to large mitochondrial protein aggregates. The appearance of these aggregates was paralleled by increased production of reactive oxygen species (ROS), inflammatory signals, cell death, and renal fibrosis. This new disease expands the gamut of etiologies of tubuloglomerular disease.

METHODS

Full details of the methods can be found in Supplemental Material.

Patients

Members of two families were admitted to the National Institutes of Health Clinical Center and enrolled in clinical protocol 1-HG-0106 or 76-HG-0238. Three additional families were evaluated in Cambridge, Oxford, and London. All participating individuals or their parents gave written informed consent. All investigations, including genetic studies, were approved by the respective institutional review boards and conducted according to the principles of the Declaration of Helsinki.

The diagnosis of renal Fanconi syndrome and kidney failure was established by routine laboratory investigations of urine and blood samples. Clinical details concerning four of these five families have been published previously.^{2–10} Kidney samples were acquired from two affected individuals. One patient was biopsied at age 21 years old; another patient died at age of 65 years old due to ESRD, and the kidney was studied at autopsy. Electron microscopic studies and histologic staining were performed using established procedures.¹¹ One affected adult and one unaffected adult underwent brain ¹H-NMR spectroscopy using standard diagnostic procedures.¹²

Genetic Studies

We previously linked the locus for this trait in an extended United States family (Figure 1A, family 1) to a region on chromosome 15q.¹³ To prove linkage to the same locus, we performed additional linkage studies in our other families showing the same trait. To this end, DNA was isolated from whole blood using standard procedures, and it was genotyped with 2000 highly polymorphic STS markers by deCODE Genetics (Iceland) for families 3–5 or commercially available single-nucleotide polymorphism chips (Affymetrix) for

Significance Statement

This manuscript describes a novel mechanism of renal tubular damage and CKD involving the formation of unique intramitochondrial protein aggregates. The disease results from monoallelic mutations in the gene encoding glycine amidinotransferase (*GATM*), a proximal tubular enzyme in the creatine biosynthetic pathway. All disease-related *GATM* mutations create an additional interaction interface within the *GATM* protein, promoting its linear aggregation. Aggregate-containing mitochondria in proximal tubular cells are associated with elevated production of reactive oxygen species, initiation of an inflammatory response, and increased cell death. These data establish a link between intramitochondrial *GATM* aggregates, renal Fanconi syndrome, and CKD.

family 2 (Figure 1A). Multipoint parametric linkage analysis was performed using established procedures for families 2–5.¹¹ Initial gene discovery was performed by either targeted capture and next generation sequencing (The Eastern Sequence and Informatics Hub, University of Cambridge, Cambridge, United Kingdom) or whole-exome sequencing (SeqWright, Inc., Houston, TX) in six affected individuals from four of our families. Recognized sequence variants within the linked region were examined for segregation in all available affected and unaffected family members and confirmed by Sanger sequencing. Observed novel sequence variants were assessed for uniqueness and evolutionary conservation in various species. Public databases (dbSNP, 1000 Genomes, and exome database) were also interrogated.

Renal Proximal Tubular Cell Model and Kidney Imaging

A permanently transfected, inducible renal proximal tubular cell line derived from LLC-PK1 cells was created for each patient *GATM* mutation using recombinant technology. LLC-PK1 cells are an established model, and they reliably express many properties of the renal proximal tubule.¹¹ For *in situ* immunolabeling, subcellular studies, metabolic studies, expression studies, and electron microscopy, cells and tissues were prepared and investigated using established procedures (for information on antibodies, please see Supplemental Table 1). Specifically, the renal and intracellular localization of *GATM* was studied. Changes in expression of relevant genes were studied using established real time PCR technology (for primer sequences, please see Supplemental Table 2).

Gatm Knockout Mice

All animal experiments were performed according to the guidelines for the care and use of laboratory animals published by the US National Institutes of Health, and they were approved by the local councils for animal care according to the German law for animal care. We previously generated *Gatm* knockout mice to study the biochemical function of this mitochondrial protein.¹⁴ Mutant mice were viable, and they were without detectable gross phenotypic defects but dystrophic. Urinary metabolites were assessed in knockout and control mice using established analytic procedures.

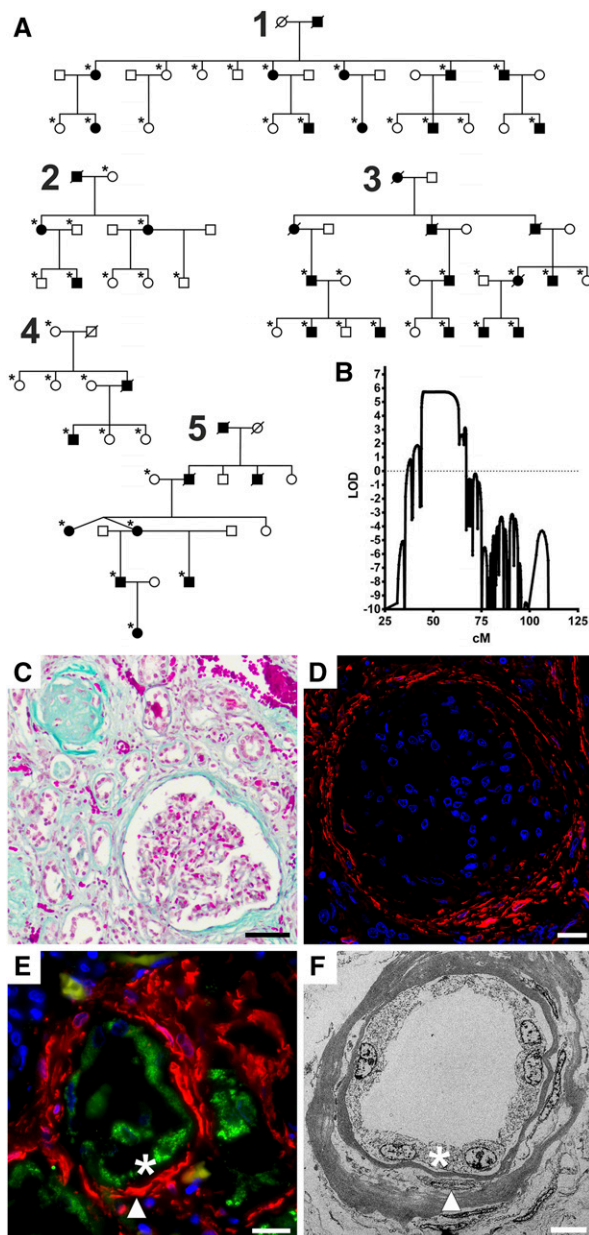


Figure 1. Pedigrees of families with autosomal dominant renal Fanconi syndrome and kidney failure and kidney specimens with signs of renal fibrosis. (A) Pedigrees of families with renal Fanconi syndrome and kidney failure. Squares indicate men, and circles indicate women. A black symbol indicates that the person is affected; deceased individuals are drawn with a diagonal line through the symbol. An asterisk indicates that the person contributed to linkage and sequencing studies. Note the *de novo* “appearance” of the disease in family 4. (B) Multipoint parametric linkage analysis for families 3–5 for chromosome 15. The y axis shows the logarithm (base 10) of odds (LOD) score, and the x axis gives the genetic distance in centimorgan. Note significant linkage (LOD score >3) in the region of 40–60 cM. (C) Masson–Goldner staining of a postmortem kidney specimen from a patient with renal Fanconi and kidney failure. Connective tissue is stained light green. This specimen shows the highly fibrotic

Structural Studies

To test the hypothesis of mutation-mediated aggregation of GATM, we performed molecular dynamics simulations on the wild-type monomer and the four mutants. Modeling of possible protein-protein interaction surfaces (GRAMM-X; vakser.bioinformatics.ku.edu/resources/gramm/grammx/) started with the structure of the wild-type monomer (Protein Data Bank ID code 1JDW).

Statistical Methods

Data are presented as the mean \pm SEM, and they were analyzed using one-way ANOVA or *t* test if not specified otherwise. For all analyses, if not stated otherwise, a *P* value of 0.05 was accepted to indicate statistical significance. Statistical analysis was performed using GraphPad Prism 5, OriginPro, and SPSS software.

RESULTS

Clinical Studies

All affected individuals from five extended families (Figure 1A) exhibited an autosomal dominant form of CKD. During childhood, all patients developed a renal Fanconi syndrome with glucosuria, hyperphosphaturia, generalized hyperaminoaciduria, low molecular weight proteinuria, and metabolic acidosis but without debilitating rickets or bone deformities. As an example, at age 18 months old, the youngest affected child studied exhibited laboratory findings typical of renal Fanconi syndrome but no glomerular compromise (Supplemental Table 3). During late adolescence or adulthood, increased plasma creatinine became apparent, and patients developed renal fibrosis and kidney failure, with the need for transplant or dialysis in the third to sixth decade of life. A graph illustrating the decline in kidney function in relation to age

terminal kidney morphology of the disease. The cortex is shrunken and contains very few proximal tubules. Most glomeruli as well as the tubules are atrophic and fibrotic (upper left corner), and some appear intact (lower right corner). Scale bar, 50 μ m. (D) Immunofluorescence of same specimen as in C. α -Smooth muscle actin (a marker for myofibroblasts) is red, and nuclei are blue. The Bowman capsule of the glomerulus contains myofibroblasts (red), which suggests that the kidney damage is not restricted to proximal tubules during the final stage of the disease. Scale bar, 20 μ m. (E) Immunofluorescence of same specimen as in C. Glycine amidinotransferase (GATM) is green, α -smooth muscle actin (a marker for myofibroblasts) is red, and nuclei are blue. The picture shows a proximal tubule with GATM-positive epithelium (asterisk). Several layers of myofibroblasts (arrowhead) surround the tubule. Scale bar, 20 μ m. (F) Electron microscopy of same specimen as in C. Most tubules show an extremely thick basal membrane containing myofibroblasts (arrowhead). Tubular epithelium is marked by an asterisk. Scale bar, 7 μ m.

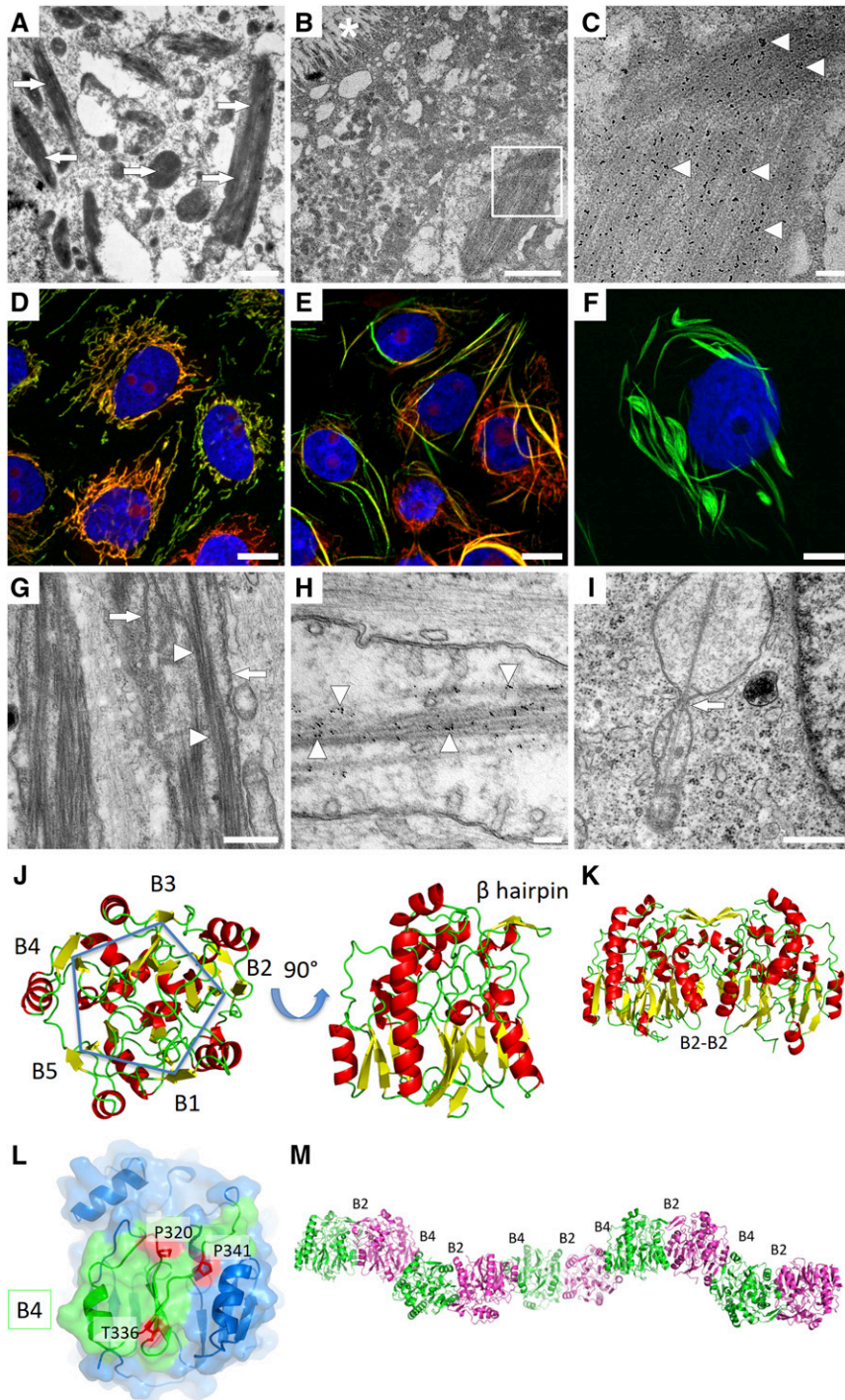


Figure 2. Mutant GATM proteins form intramitochondrial filaments due to a mutation-induced additional interaction site that allows linear aggregation of GATM dimers. (A) Electron microscopy of a proximal tubular cell from a patient's biopsy showing giant mitochondria with deposits (arrows). Scale bar, 1 μ m. (B) Glycine amidinotransferase (GATM) immunogold electron microscopy of a proximal tubular cell with an enlarged, filament-containing mitochondrion from a patient's biopsy. Asterisk indicates proximal tubule brush border membrane. Scale bar, 2 μ m. (C) Higher magnification of B (white square). Note the packed linear deposits with 6-nm GATM-specific gold particles attached (arrowheads). Scale bar, 200 nm. (D) Immunofluorescence of LLC-PK1 renal proximal tubular cells with induced expression (3 days) of wild-type GATM (green). Normal mitochondria are in red (Mitotracker), and nuclei are in blue. Scale bar, 20 μ m. (E) Immunofluorescence of LLC-PK1 cells with induced expression (3 days) of mutant GATM (T336A; green) and abnormal mitochondria (red). Nuclei are in blue. Scale bar, 20 μ m. (F) Immunofluorescence of LLC-PK1 cells with induced expression (9 weeks) of mutant GATM (green) causing large deposits. Nucleus is in blue. Scale bar, 10 μ m. (G) Electron microscopy of an LLC-PK1 cell

is shown in Supplemental Figure 1. Premature deaths due to compromised glomerular kidney function occurred in several families. No extrarenal clinical findings were noted.

Genetic Analyses

In all six affected individuals initially studied, sequencing of all genes within the linked locus on chromosome 15 (Figure 1B) showed mutations in a single gene identified as *GATM* encoding the “glycine amidinotransferase.” Subsequent sequencing of all 28 clinically affected individuals showed that each had one heterozygous missense mutation in *GATM*. We identified four previously unreported heterozygous missense mutations of evolutionary conserved amino acid residues in *GATM* (c.958C>T, p.P320S; c.1006A>G, p.T336A; c.1007C>T, p.T336I; c.1022C>T, p.P341L) (Supplemental Figure 2). In each family, one variant segregated with the disorder and was fully penetrant. None of the unaffected family members carried any of these *GATM* mutations. One family showed a *de novo* heterozygous mutation in affected offspring confirmed by haplotype analysis, which was passed on to the next generation (Figure 1A, family 4).

Histologic Examinations

Patients' biopsies showed the morphologic correlate of kidney fibrosis on routine staining (Figure 1, C–F, Supplemental Figure 3). In normal kidneys, *GATM* was found in mitochondria of proximal tubules, particularly in the early segments (Supplemental Figure 4).¹⁵ In a patient's kidney biopsy, electron microscopy and *GATM*-specific immunogold labeling of renal proximal tubules revealed drastically enlarged mitochondria containing pathologic *GATM* protein aggregates (Figure 2, A–C).

To further explore the pathophysiologic mechanisms of this particular mitochondrial phenotype, we overexpressed wild-type or mutant *GATM* in a renal proximal tubule cell line, LLC-PK1 (Supplemental Figure 5). Normal mitochondrial morphology was observed in cells expressing wild-type *GATM*, but abnormal and elongated mitochondria were observed in the cells expressing the *GATM* T336A mutant

(Figure 2, D–F, Supplemental Figure 6). Similar findings were present in cells transfected with *GATM* mutants T336I, P341L, and P320S (Supplemental Figure 7). Immunogold electron microscopy of cells overexpressing mutant *GATM* showed drastically enlarged mitochondria containing *GATM*-positive fibrillary aggregates, similar to the deposits observed in proximal tubules of patients' biopsies (Figure 2, G–I).

Structural Studies

We performed *in silico* structural studies of *GATM*, which contains ten x-ray crystallographic structures in the Protein Data Bank.¹⁶ The 423-amino acid *GATM* protein is built around a central core formed by five antiparallel β -sheets (B1–B5) disposed around a fivefold axis of symmetry. Such a structure is potentially prone to protein-protein aggregation due to the presence of the five solvent-exposed β -sheets. In addition to the domain of fivefold symmetry, the *GATM* protein hosts one additional domain composed of four α -helices and a β -hairpin involved in formation of the wild-type dimer. Assembly of the physiologic *GATM* dimer involves the two facing β -sheets (B2) disposed in parallel with an angle of approximately 45° with respect to each other, harboring the catalytic enzymatic activity domain (Figure 2, J and K).

The four disease-related mutations involve three amino acids conserved through evolution (Supplemental Figure 2) (*i.e.*, Pro320, Pro341, and Thr336). All three are located on the surface around sheet B4, which is located opposite to the B2 surface (Figure 2, K and L). Thus, these mutations could impair the proper folding of the B4 surface. In fact, structure simulations of these four *GATM* mutants predicted increased mobility of the same region for each of them, predisposing the mutated B4 region to form an additional interaction site. Specifically, the presence of two opposite dimerization surfaces, B2 and B4, would support the formation of linear multimers, with each mutant *GATM* monomer linked to two protein partners by two dimerization interfaces (*i.e.*, the existing “physiological” B2–B2 and the “*de novo*” pathologic B4–B4 interface) (Figure 2M).

overexpressing the T336A mutant. Within the mitochondrial matrix, *GATM* filaments were aligned in a parallel manner (arrowheads). Cristae are marked by arrows. Scale bar, 500 nm. (H) Immunogold electron microscopy of mutant *GATM* (T336A) in LLC-PK1 cells. Intra-mitochondrial gold particles attached to linear long aggregates (arrowheads) indicate that *GATM* comprises these deposits. Scale bar, 100 nm. (I) Electron microscopy of LLC-PK1 cells overexpressing the P341L mutant in LLC-PK1 cells. A *GATM* filament appears to prevent mitochondrial fission (arrow). Scale bar, 500 nm. (J) Wild-type *GATM* in two orientations rotated by 90° around the horizontal axis colored by secondary structures: yellow β -sheets, green loops, and red α -helices. In the left orientation, the fivefold symmetry with the five β -sheets B1–B5 is visible. In the right orientation, the β -hairpin involved in wild-type homodimer formation becomes visible. (K) The wild-type homodimer is stabilized by interaction of β -sheets B2. (L) Mutated *GATM*. Surface of the B4 module (green) shows the mutated amino acids in red. Remainder of *GATM* is blue. Localization of all observed mutations (p.P320S, p.T336A, p.T336I, and p.P341L) on the same surface leads to the appearance of a novel additional interaction site. (M) Proposed disease mechanism in which the creation of an additional mutation-related novel interaction site in the B4 module can lead to aggregation of *GATM* multimers instead of the physiologic homodimer; B2 denotes physiologic interaction site forming enzymatically active *GATM*. B4 denotes additional interaction site opposite the B2 module mediating longitudinal *GATM* aggregation. Monomers carrying the mutation are shown in green and cyan, respectively.

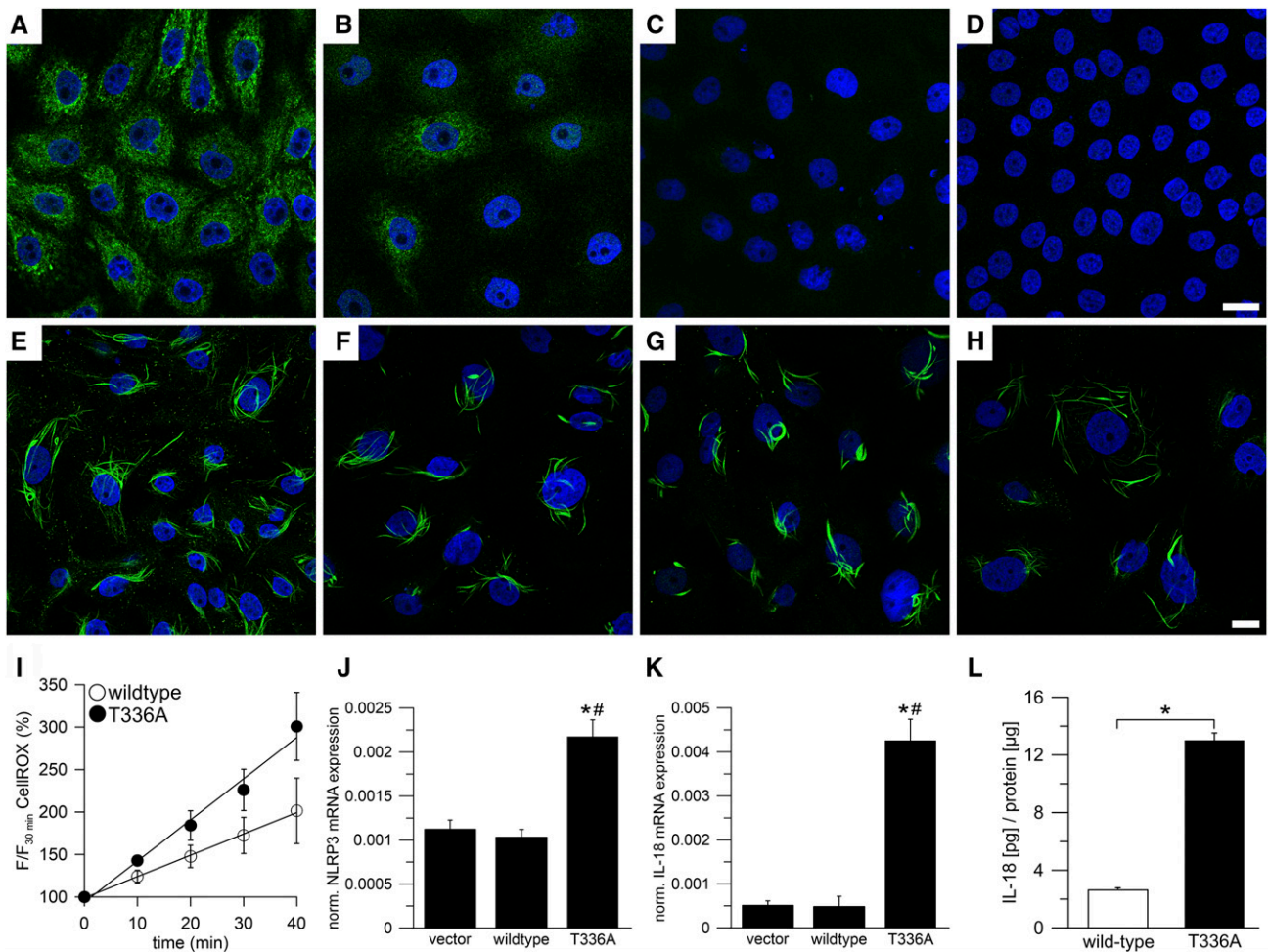


Figure 3. Intramitochondrial filaments of mutant GATM escape degradation and are associated with increased ROS production and activation of the NLRP3 inflammasome. (A–D) LLC-PK1 cells, induced with tetracycline for 2 weeks, overexpressed wild-type glycine amidinotransferase (GATM). Induction was discontinued to stop further overexpression. GATM was immunolabeled immediately after (A) discontinuing tetracycline or (B) 4, (C) 6, and (D) 8 weeks. At week 4, the GATM signal (green) was very faint, and at week 6, GATM was no longer detected. Nuclei are in blue. Scale bar, 20 μ m. (E–H) Protocol is the same as in A–D but with LLC-PK1 cells overexpressing the T336A mutant. Within 8 weeks, the cells were not able to degrade GATM deposits and giant mitochondria. Scale bar, 20 μ m. (I) Live cell imaging of mitochondrial reactive oxygen species (ROS) production in LLC-PK1 cells overexpressing wild-type GATM ($n=6$) or the T336A mutant ($n=6$). ROS production rate was measured with the ROS cell-permeant dye CellROX Deep Red. The slopes of the linear regression curves were significantly different (analysis of covariance; $P<0.01$). (J and K) Real time PCR in LLC-PK1 vector control cells (vector), cells overexpressing wild-type GATM (wild type), and the T336A mutant (T336A); $n=20$ dishes for each group (mean \pm SEM). Values were normalized to β -actin mRNA expression. (J) Real time PCR of the inflammasome component NLRP3. *Significantly different from vector control cells (ANOVA; Bonferroni test; $P<0.001$); #significantly different from wild-type GATM-expressing cells ($P<0.001$). (K) Real time PCR of the profibrotic cytokine IL-18. *Significantly different from vector control cells (ANOVA; Bonferroni test; $P<0.001$); #significantly different from wild-type GATM-expressing cells ($P<0.001$). (L) IL-18 ELISA in total cell lysates of LLC-PK1 cells overexpressing wild-type GATM ($n=3$) or the T336A mutant ($n=3$). Data were normalized to total protein content. *Overexpression of the T336A mutant led to increased IL-18 synthesis (unpaired; two-sided t test; $P=0.001$).

Gatm^{-/-} Mouse Studies

We used *Gatm*^{-/-} mice to determine whether mitochondrial GATM haploinsufficiency (*i.e.*, decreased GATM activity) was likely to have caused our families' renal Fanconi syndrome. No aminoaciduria or glucosuria was observed in these mice (Supplemental Figure 8), indicating that lack of *Gatm* did not significantly affect renal proximal tubular function. Rather, we propose that mutant GATM proteins within mitochondria

trigger a pathologic cascade inside and outside the proximal tubules, resulting in our patients' signs and symptoms.

Intramitochondrial Deposits Impair Mitochondrial Degradation and Elicit an Inflammatory Response

In a next set of experiments, we investigated mitochondrial turnover in cells overexpressing mutant GATM. Electron micrographs of these cells indicated that the fibrillary GATM deposits

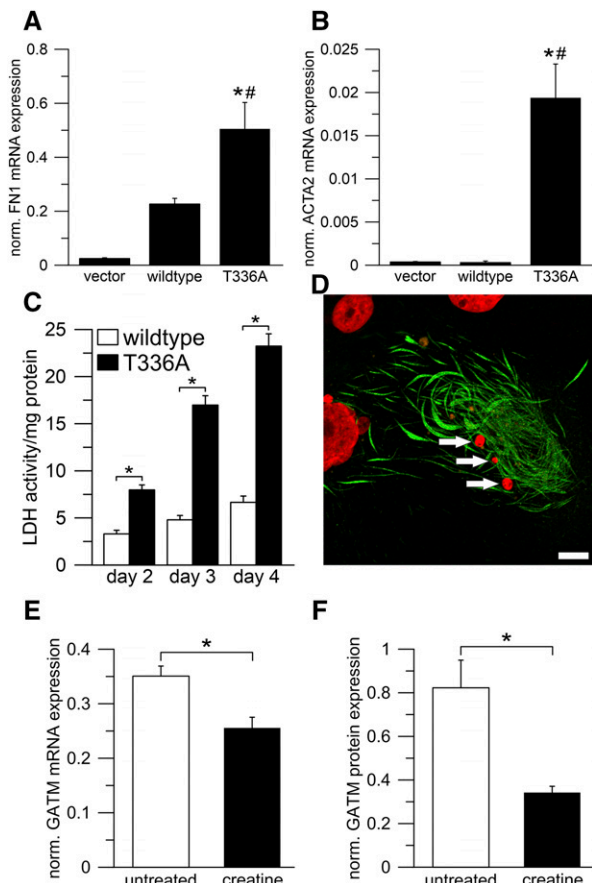


Figure 4. Expression of mutant GATM in epithelial cells results in enhanced transcription of fibronectin and smooth muscle actin and increases the rate of cell death. Dietary creatine supplementation can be used to suppress GATM expression. (A and B) Real time PCR in LLC-PK1 vector control cells (vector), cells overexpressing wild-type glycine amidinotransferase (GATM; wild type), and the T336A mutant (T336A); $n=20$ dishes for each group (mean \pm SEM). Values were normalized to β -actin expression. (A) Real time PCR of fibronectin 1 (FN1). Values of vector control cells were not different from wild-type GATM-expressing cells ($P=0.05$). *Significantly different from vector control cells (ANOVA; Bonferroni test; $P<0.001$); #significantly different from wild-type GATM-expressing cells ($P=0.003$). (B) Real time PCR of α -smooth muscle actin 2 (ACTA2). *Significantly different from vector control cells (ANOVA; Bonferroni test; $P<0.001$); #significantly different from wild-type GATM-expressing cells ($P<0.001$). (C) Lactate dehydrogenase (LDH) release as a measure of cell death in LLC-PK1 cells overexpressing wild-type GATM ($n=3$) or the T336A mutant ($n=3$). After induction (3 weeks), the cell medium remained unchanged, and samples were taken on days 2–4. ANOVA with *post hoc t* tests corrected for multiple testing by the Bonferroni method; P values were 0.004 (day 2), <0.0001 (day 3), and <0.0001 (day 4). *Significantly different from wild-type GATM-expressing cells. (D) Cell death in LLC-PK1 cells overexpressing the T336A mutant (induced for 7 weeks). The remains of a dead cell with giant mitochondria (green). The nucleus (red) is fragmented (arrows), indicating cell death. Scale bar, 10 μ m. (E and F) Effect of oral creatine supplementation on GATM expression. Wild-type mice were supplemented with 1% creatine in

might impair mitochondrial fission and thus, mitochondrial degradation (Figure 2I). Indeed, overexpression of mutant GATM led to a reduced mitochondrial turnover rate in our cell model. This was evidenced by the presence of GATM-positive enlarged mitochondria even 8 weeks after induction of GATM T336A expression was discontinued (Figure 3, A–H).

Furthermore, we explored possible links between mitochondrial GATM protein deposits and pathways inducing tubular damage and renal fibrosis. The mitochondrial phenotype in our cell model was associated with an increased production of ROS (Figure 3I). Excess ROS generation leads to oxidative stress and triggers—in concert with other factors—the inflammasome.^{17–20} In fact, LLC-PK1 cells carrying mitochondrial GATM deposits showed significantly elevated mRNA expression of both the inflammasome component NLRP3 and IL-18, a cytokine known to promote renal fibrosis (Figure 3, J and K).^{21,22} IL-18 protein was also elevated as measured by ELISA (Figure 3L). Moreover, those cells exhibited increased fibronectin and smooth muscle actin mRNA levels (Figure 4, A and B) as well as an increased rate of cell death (Figure 4, C and D). These findings strongly suggest that mitochondrial GATM aggregates led to activation of components of the inflammasome and release of profibrotic factors, thereby providing a plausible pathogenic link between heterozygous GATM mutations, kidney fibrosis, and renal failure.

Potential Treatment

Because mutant GATM protein resulted in pathogenic intramitochondrial deposits in renal proximal tubular cells, we investigated means to reduce GATM production. GATM expression was reported to be negatively feedback regulated by creatine in rats,²³ and therefore, we supplemented wild-type mice with 1% creatine in their drinking water for 1 week. This protocol reduced renal GATM mRNA expression by 27% and GATM protein by 58% (Figure 4, E and F, Supplemental Figure 9), corroborating previous findings.²³ Hence, creatine supplementation could serve as an intervention to suppress the endogenous production of mutated GATM protein and retard the formation of deleterious mitochondrial deposits.

DISCUSSION

CKD affects 8%–16% of the adult population and comprises heterogeneous disorders of unknown etiology affecting kidney structure and function.^{1,24,25} Here, we provide genetic, histologic, cell biologic, and structural evidence for the association between monoallelic GATM mutations and a genetic disorder

their drinking water ($n=4$) for 1 week; control mice received tap water ($n=4$). *Significantly different from untreated mice. Renal GATM mRNA and protein expression were determined using (E) real time PCR and (F) Western blot. Creatine supplementation led to a reduction of mRNA and protein expression (unpaired, two-sided *t* tests; $P=0.01$ and $P=0.03$, respectively). Values are normalized to β -actin mRNA or total protein expression.

characterized by renal Fanconi syndrome and progressive kidney failure.

GATM encodes the mitochondrial enzyme “glycine amidinotransferase” (“L-arginine:glycine amidinotransferase,” which is also known as AGAT), which catalyzes the transfer of a guanidino group from L-arginine to glycine, resulting in guanidinoacetic acid, the immediate precursor of creatine.^{16,26,27} *GATM* is expressed most prominently in kidney, liver, pancreas, and brain. Recessive loss-of-function mutations of *GATM* result in “cerebral creatine deficiency syndrome,” a rare inborn error of creatine synthesis characterized by severe neurologic impairment.^{12,28} A *Gatm*^{-/-} mouse model also showed neurologic symptoms caused by creatine deficiency¹⁴ but normal kidney function (Supplemental Figure 8). In contrast to patients with “cerebral creatine deficiency syndrome,” none of our patients showed extrarenal symptoms. The one patient studied by brain ¹H-NMR spectroscopy had a normal creatine peak (Supplemental Figure 10), indicating that the disorder in our patients was not related to creatine deficiency.

Histologic examinations of patients’ kidney biopsies revealed a dramatic mitochondrial phenotype associated with *GATM* mutations. Mitochondria of proximal tubular cells were drastically enlarged and filled with filament-like deposits. This phenotype was also observed in an LLC-PK1 cell model overexpressing *GATM* mutants. Immunogold studies on a patient biopsy and LLC-PK1 cells showed that these deposits were composed of mutant *GATM* protein, and *in silico* structural studies provided an explanation. Heterozygous *GATM* mutations in a particular region of the enzyme led to the creation of an additional *de novo* interaction surface, causing intramitochondrial “multimeric” aggregation. This functional effect of the mutations was in line with the dominant inheritance of the disease.

Mitochondrial fission results in smaller mitochondria and thereby, facilitates removal and degradation of aged mitochondria by mitophagy.²⁹ Intramitochondrial aggregates of mutant *GATM* apparently impaired mitochondrial division, leading to pathologically enlarged and aged mitochondria that could no longer be removed by mitophagy. In our LLC-PK1 cell model, mitochondria with *GATM* deposits were still present even 8 weeks after *GATM* mRNA expression was discontinued. The long persistence of deposits contrasted with the physiologic turnover rate of mitochondria, which was estimated to be 2–4 weeks.²⁹ These data suggest that the long fibrillary deposits of mutant *GATM*, once aggregated, escape cellular degradation, prevent mitochondrial fission, and lead to enlarged, aged mitochondria.

Aged mitochondria as well as nondegradable deposits and crystalline structures are known to trigger an inflammatory response and activate the NLRP3 inflammasome.^{17,18,30–33} In agreement with these reports, the appearance of mutant *GATM* aggregates in our cell model was paralleled by enhanced inflammatory markers: NLRP3 and its downstream signaling molecule IL-18 were strongly elevated. We also found evidence of increased ROS production in mutated cells. Mitochondria are a major source of intracellular ROS, and excess ROS generation is known

to lead to oxidative stress and trigger the inflammasome as well.^{34,35} In addition, overexpression of mutant *GATM* led to an increased rate of cell death and enhanced expression of the fibrosis marker fibronectin and smooth muscle actin. In line with this profound *in vitro* cytopathologic phenotype, immunofluorescence studies in kidney biopsies from our patients revealed significant interstitial fibrosis with myofibroblasts surrounding renal tubules and thickening of tubular basement membranes, eventually leading to kidney failure.^{20,21,33}

Taken together, we provide evidence that intramitochondrial aggregates consisting of mutated *GATM* protein are causative for an autosomal dominant form of renal Fanconi syndrome and CKD. This finding expands the spectrum of disorders associated with pathologic protein aggregates. The disease also illustrates the critical role that mitochondria can play in initiating devastating profibrotic signaling cascades. This may have implications for understanding the pathophysiology of CKD. An association of genetic variation in the *GATM* gene with plasma creatinine levels was previously suggested by genome-wide association studies.^{36–38}

Cohorts of patients with kidney failure or renal insufficiency deserve up to date genetic diagnostic procedures, with attention to *de novo* mutations. Sequencing of *GATM* should be considered in patients with kidney failure, particularly adults with or without familial occurrence. Moreover, kidney biopsies that do not yield a diagnosis on the basis of standard histology should be considered for ultrastructural analysis, with consideration of tubular pathology rather than an evaluation limited to the glomerulus and interstitium. Finally, for patients with autosomal dominant *GATM* mutations, only 50% of the *GATM* protein is abnormal, and biosynthesis of creatine is negatively feedback regulated by its product.²³ Hence, creatine supplementation could serve as a pharmacologic intervention to suppress the endogenous production of mutated *GATM* protein, which triggers the cascade, leading ultimately to kidney fibrosis and failure.

ACKNOWLEDGMENTS

We are indebted to Dr. Robert L. Nussbaum, Dr. Donna M. Krasnewich, Dr. Edward B. Blau, the late Dr. Oliver M. Wrong, and the late Dr. Norman J. Siegel for their significant support, mentoring, expert discussions, and advice. We are grateful to all of our patients and their families for their very kind and significant engagement.

Funding for this study was provided by Deutsche Forschungsgemeinschaft grant SFB699 (to M.R., J.R., and R.W.), St. Peter’s Trust for Kidney, Bladder & Prostate Research (E.D.K., H.C.S., S.B.W., D.B., and R.K.), Swedish Society for Medical Research (R.S.), Italian Government Project PRIN NOXSS x-Ray Single Shots of Nano Objects grant 2012Z3N9R9 (to M.M.), the Lowe Syndrome Trust (D.B., R.J.U., and R.K.), European Union FP7 grant 2012-305608 “European Consortium for High-Throughput Research in Rare Kidney Diseases (EURenOmics)” (to D.B., R.J.U., and R.K.), Kids Kidney Research (D.B. and R.K.), the Moorhead Trust (D.B. and R.K.), and the David and Elaine Potter Charitable Foundation (R.K.). This work was also

supported, in part, by Wellcome Trust Centre award 090532/Z/09/Z (to A.C.-S. and B.D.) and the Intramural Research Program of the National Human Genome Research Institute (U.-L.K. and W.A.G.).

W.A.G., R.J.U., R.W., and R.K. (overall responsible) vouch for the data and the analysis.

DISCLOSURES

C.-U.C. received lecture fees from Bristol-Myers Squibb/Pfizer.

REFERENCES

- Jha V, Garcia-Garcia G, Iseki K, Li Z, Naicker S, Plattner B, et al.: Chronic kidney disease: Global dimension and perspectives. *Lancet* 382: 260–272, 2013
- Dent CE, Harris H: The genetics of cystinuria. *Ann Eugen* 16: 60–87, 1951
- Luder J, Sheldon W: A familial tubular absorption defect of glucose and amino acids. *Arch Dis Child* 30: 160–164, 1955
- Sheldon W, Luder J, Webb B: A familial tubular absorption defect of glucose and amino acids. *Arch Dis Child* 36: 90–95, 1961
- Smith R, Lindenbaum RH, Walton RJ: Hypophosphataemic osteomalacia and Fanconi syndrome of adult onset with dominant inheritance. Possible relationship with diabetes mellitus. *Q J Med* 45: 387–400, 1976
- Brenton DP, Isenberg DA, Cusworth DC, Garrod P, Krywawych S, Stamp TC: The adult presenting idiopathic Fanconi syndrome. *J Inher Metab Dis* 4: 211–215, 1981
- Patrick A, Cameron JS, Ogg CS: A family with a dominant form of idiopathic Fanconi syndrome leading to renal failure in adult life. *Clin Nephrol* 16: 289–292, 1981
- Wen SF, Friedman AL, Oberley TD: Two case studies from a family with primary Fanconi syndrome. *Am J Kidney Dis* 13: 240–246, 1989
- Long WS, Seashore MR, Siegel NJ, Bia MJ: Idiopathic Fanconi syndrome with progressive renal failure: A case report and discussion. *Yale J Biol Med* 63: 15–28, 1990
- Harrison NA, Bateman JM, Ledingham JG, Smith R: Renal failure in adult onset hypophosphatemic osteomalacia with Fanconi syndrome: A family study and review of the literature. *Clin Nephrol* 35: 148–150, 1991
- Klootwijk ED, Reichold M, Helip-Wooley A, Tolaymat A, Broeker C, Robinette SL, et al.: Mistargeting of peroxisomal EHHADH and inherited renal Fanconi's syndrome. *N Engl J Med* 370: 129–138, 2014
- Joncquel-Chevalier Curt M, Voicu PM, Fontaine M, Dessein AF, Porchet N, Mention-Mulliez K, et al.: Creatine biosynthesis and transport in health and disease. *Biochimie* 119: 146–165, 2015
- Lichter-Konecki U, Broman KW, Blau EB, Konecki DS: Genetic and physical mapping of the locus for autosomal dominant renal Fanconi syndrome, on chromosome 15q15.3. *Am J Hum Genet* 68: 264–268, 2001
- Choe CU, Nabuurs C, Stockebrand MC, Neu A, Nunes P, Morellini F, et al.: L-arginine:glycine amidinotransferase deficiency protects from metabolic syndrome. *Hum Mol Genet* 22: 110–123, 2013
- McGuire DM, Gross MD, Elde RP, van Pilsum JF: Localization of L-arginine-glycine amidinotransferase protein in rat tissues by immunofluorescence microscopy. *J Histochem Cytochem* 34: 429–435, 1986
- Humm A, Fritsche E, Steinbacher S, Huber R: Crystal structure and mechanism of human L-arginine:glycine amidinotransferase: A mitochondrial enzyme involved in creatine biosynthesis. *EMBO J* 16: 3373–3385, 1997
- Halle A, Hornung V, Petzold GC, Stewart CR, Monks BG, Reinheckel T, et al.: The NALP3 inflammasome is involved in the innate immune response to amyloid-beta. *Nat Immunol* 9: 857–865, 2008
- Dostert C, Pétrilli V, Van Bruggen R, Steele C, Mossman BT, Tschopp J: Innate immune activation through Nalp3 inflammasome sensing of asbestos and silica. *Science* 320: 674–677, 2008
- Vilaysane A, Chun J, Seamone ME, Wang W, Chin R, Hirota S, et al.: The NLRP3 inflammasome promotes renal inflammation and contributes to CKD. *J Am Soc Nephrol* 21: 1732–1744, 2010
- Anders HJ, Schaefer L: Beyond tissue injury-damage-associated molecular patterns, toll-like receptors, and inflammasomes also drive regeneration and fibrosis. *J Am Soc Nephrol* 25: 1387–1400, 2014
- Liang D, Liu HF, Yao CW, Liu HY, Huang-Fu CM, Chen XW, et al.: Effects of interleukin 18 on injury and activation of human proximal tubular epithelial cells. *Nephrology (Carlton)* 12: 53–61, 2007
- Bani-Hani AH, Leslie JA, Asanuma H, Dinarello CA, Campbell MT, Meldrum DR, et al.: IL-18 neutralization ameliorates obstruction-induced epithelial-mesenchymal transition and renal fibrosis. *Kidney Int* 76: 500–511, 2009
- McGuire DM, Gross MD, Van Pilsum JF, Towle HC: Repression of rat kidney L-arginine:glycine amidinotransferase synthesis by creatine at a pretranslational level. *J Biol Chem* 259: 12034–12038, 1984
- Zhou D, Liu Y: Renal fibrosis in 2015: Understanding the mechanisms of kidney fibrosis. *Nat Rev Nephrol* 12: 68–70, 2016
- Bohle A, Mackensen-Haen S, von Gise H: Significance of tubulointerstitial changes in the renal cortex for the excretory function and concentration ability of the kidney: A morphometric contribution. *Am J Nephrol* 7: 421–433, 1987
- Guthmiller P, Van Pilsum JF, Boen JR, McGuire DM: Cloning and sequencing of rat kidney L-arginine:glycine amidinotransferase. Studies on the mechanism of regulation by growth hormone and creatine. *J Biol Chem* 269: 17556–17560, 1994
- Wyss M, Kaddurah-Daouk R: Creatine and creatinine metabolism. *Physiol Rev* 80: 1107–1213, 2000
- Item CB, Stöckler-Ipsiroglu S, Stromberger C, Mühl A, Alessandri MG, Bianchi MC, et al.: Arginine:glycine amidinotransferase deficiency: The third inborn error of creatine metabolism in humans. *Am J Hum Genet* 69: 1127–1133, 2001
- Terman A, Kurz T, Navratil M, Arriaga EA, Brunk UT: Mitochondrial turnover and aging of long-lived postmitotic cells: The mitochondrial-lysosomal axis theory of aging. *Antioxid Redox Signal* 12: 503–535, 2010
- Nakahira K, Haspel JA, Rathinam VA, Lee SJ, Dolinay T, Lam HC, et al.: Autophagy proteins regulate innate immune responses by inhibiting the release of mitochondrial DNA mediated by the NALP3 inflammasome. *Nat Immunol* 12: 222–230, 2011
- Duewell P, Kono H, Rayner KJ, Sirois CM, Vladimer G, Bauernfeind FG, et al.: NLRP3 inflammasomes are required for atherogenesis and activated by cholesterol crystals. *Nature* 464: 1357–1361, 2010
- Knauf F, Asplin JR, Granja I, Schmidt IM, Moeckel GW, David RJ, et al.: NALP3-mediated inflammation is a principal cause of progressive renal failure in oxalate nephropathy. *Kidney Int* 84: 895–901, 2013
- Mulay SR, Kulkarni OP, Rupanagudi KV, Migliorini A, Darisipudi MN, Vilaysane A, et al.: Calcium oxalate crystals induce renal inflammation by NLRP3-mediated IL-1 β secretion. *J Clin Invest* 123: 236–246, 2013
- Fougeray S, Pallet N: Mechanisms and biological functions of autophagy in diseased and ageing kidneys. *Nat Rev Nephrol* 11: 34–45, 2015
- Abais JM, Xia M, Zhang Y, Boini KM, Li PL: Redox regulation of NLRP3 inflammasomes: ROS as trigger or effector? *Antioxid Redox Signal* 22: 1111–1129, 2015
- Köttgen A, Glazer NL, Dehghan A, Hwang SJ, Katz R, Li M, et al.: Multiple loci associated with indices of renal function and chronic kidney disease. *Nat Genet* 41: 712–717, 2009
- Park H, Kim HJ, Lee S, Yoo YJ, Ju YS, Lee JE, et al.: A family-based association study after genome-wide linkage analysis identified two genetic loci for renal function in a Mongolian population. *Kidney Int* 83: 285–292, 2013
- Pattaro C, Teumer A, Gorski M, Chu AY, Li M, Mijatovic V, et al.: ICBP Consortium; AGEN Consortium; CARDIOGRAM; CHARGE-Heart Failure Group; ECHOGen Consortium: Genetic associations at 53 loci highlight cell types and biological pathways relevant for kidney function. *Nat Commun* 7: 10023, 2016

See related editorial, "GATM Mutations Cause a Dominant Fibrillar Conformational Disease in Mitochondria—When Eternity Kills," on pages 1787–1789.

This article contains supplemental material online at <http://jasn.asnjournals.org/lookup/suppl/doi:10.1681/ASN.2017111179/-DCSupplemental>.

AFFILIATIONS

¹Medical Cell Biology, ³Institute of Functional Genomics, ⁷Department of Internal Medicine III, and ⁸Molecular and Cellular Anatomy, University Regensburg, Regensburg, Germany; ²Centre for Nephrology and ²²Genetics, Evolution and Environment, University College London, London, United Kingdom; ⁴Division of Nephrology and ⁶Department of Pediatrics and Communicable Diseases, University of Michigan, Ann Arbor, Michigan; ⁵Italian National Research Council (CNR), Institute of Biophysics, Milan, Italy; ⁹Institute of Anatomy, University of Zurich, Zurich, Switzerland; ¹⁰Department of Pathology, Yale University, New Haven, Connecticut; ¹¹NHGRI, National Institutes of Health, Bethesda, Maryland; ¹²Mayo Clinic, Jacksonville, Florida; ¹³Department of Bone and OI, Kennedy Krieger Institute, Baltimore, Maryland; ¹⁴King's College London and Guy's and St. Thomas' PET Centre, London, United Kingdom; ¹⁵Medical Physics, Guy's and St. Thomas' NHS Foundation Trust, London, United Kingdom; ¹⁶Department of Neurology, University Hamburg, Hamburg, Germany; ¹⁷Deutsches Zentrum für Neurodegenerative Erkrankungen (DZNE), Research Group Experimental Neurophysiology, Bonn, Germany, and University of Cologne, Cologne, Germany; ¹⁸Wellcome Centre for Human Genetics and ²⁰Nuffield Department of Medicine, University of Oxford, Oxford, United Kingdom; ¹⁹Department of Medical Genetics, University of Cambridge, Cambridge, United Kingdom; ²¹GeneDX, Gaithersburg, Maryland; and ²³Division of Medical Genetics, University of Pittsburgh, Pittsburgh, Pennsylvania